

## NUMERICAL SIMULATIONS OF COUPLED PROBLEMS IN A VACUUM DISJUNTOR

S. Clain<sup>1,2</sup> and J. Rodrigues<sup>1,3\*</sup>

1: CMAT - Universidade do Minho  
Campus de Gualtar  
4710 - 057 Braga

2: Departamento de Matemática e Aplicações  
Campus de Gualtar - 4710-057 Braga  
e-mail: clain@math.uminho.pt

3: Área Departamental de Matemática  
Instituto Superior de Engenharia de Lisboa  
e-mail: jrodri@dec.isel.pt

**Keywords:** Finite element method, Contact problem, Domain decomposition method, Linear elasticity, Helmotz equation, Biot-Savard

**Abstract** *In this work we carried out the modelling, the discretization and the numerical simulation of a vacuum breaker. We present a mathematical model of the multi-physical problem involving mechanical, electrical and electromagnetic phenomena. The finite element method is employed in conjunction with a technique of domain decomposition to solve the mechanical problem and the electrical problem while a direct integration of the Biot-Savart formula allows to compute an approximation of the magnetic field, hence the Lorentz-Laplace forces.*

## 1 INTRODUCTION

A vacuum circuit breaker is a device that allows the cutting of electrical power. The apparatus core is essentially constituted of two electrodes, one of them being mobile and subject to a mechanical force produced by a spring, maintaining the contact between the two electrodes (see figure 2 left). The current passing between two electrodes is determined by the extension of the contact zone and generated Lorentz-Laplace forces in areas bordering the contact, but not yet in contact. Due to the curved geometry of the electrodes, Lorentz-Laplace forces are opposite and cause the repulsion of the electrodes. When the intensity reach a critical value, the forces separate the two electrodes and the circuit is breaking. For a given intensity, the equilibrium position and the contact area result from the balance between the spring constraint and the repulsive Lorentz-Laplace deriving from the electric and magnetic fields.

To determine the equilibrium, we have to consider three sub-problems, namely, the mechanical problem, the electrical problem and the magnetic problem. Indeed (see diagram in figure 1), the spring force in conjunction with the Lorentz-Laplace force determine the displacement of the two bodies and the contact area. From the contact area, we deduce the current density distribution and the electric field. With the current density, we compute the magnetic field and we deduce the Lorentz-Laplace force with the electric and the magnetic field.

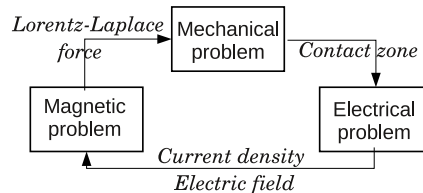


Figure 1: The circuit-breaker modelling: a coupling of three mathematical sub-problems

The goal of the present article is to present the modelling and the numerical simulation of each subgroup. In section 1, we present the multi-physical model for the circuit breaker divided in three sub-models. Section 2 is dedicated to the numerical method employed in each sub-model. We present the discretization of the mechanical problem using the finite element method coupled with the Mortar method. We also employ the finite element method to compute the electrical current assuming that the contact area is given. At last, we present the numerical method to compute the magnetic field based on the Biot and Savard formula to evaluate the Lorentz-Laplace forces. The section 3 concerns the numerical simulations for each sub-model of the vacuum circuit breaker.

## 2 MATHEMATICAL FORMULATION

We consider two electrodes in contact, as in figure 2. The bottom one is constituted by

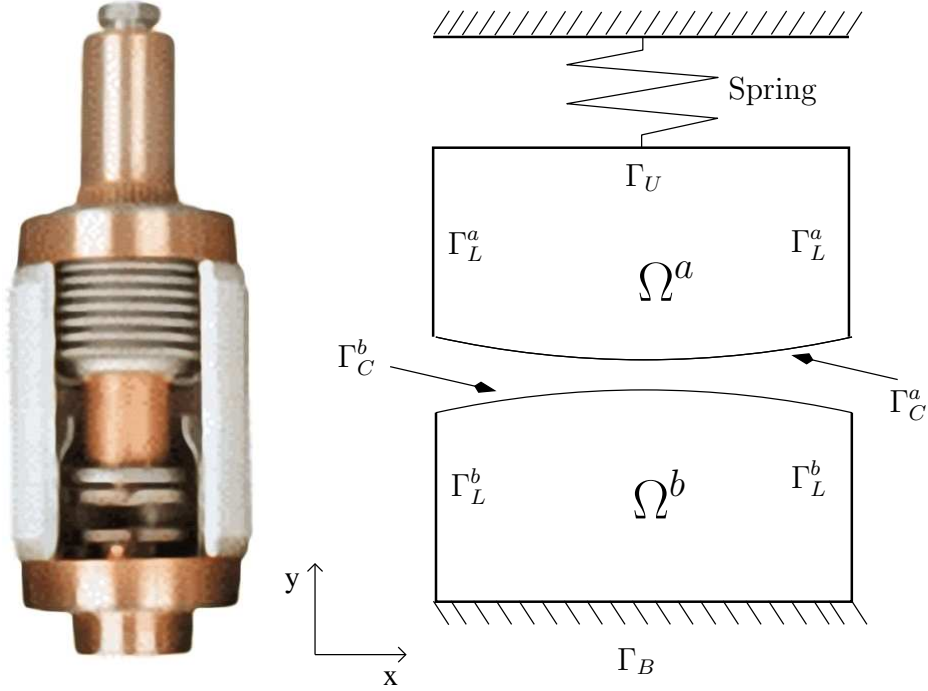


Figure 2: The circuit-breaker and the geometry

a piece of copper named  $\Omega^b$  fixed on a support foundation denoted by  $\Gamma_B$ , the interface between the electrode and its support. The lateral sides of the electrode  $\Omega^b$  (denoted by  $\Gamma_L^b$ ) are free of constraint.

A second upper electrode, characterized by domain  $\Omega^a$  is maintained in contact with  $\Omega^b$  applied a force on the upper side of  $\Omega^a$ , named  $\Gamma^U$ . To determine the force, we assume that the spring force is uniformly applied on the  $\Gamma_U$  face with a prescribed constraint. Since  $\Omega^a$  is mobile, the force will change with the displacement of  $\Omega^a$ . Like in  $\Omega^b$ , the lateral sides (denoted by  $\Gamma_L^a$ ) are free and no force or displacement are prescribed.

At last, we denote by  $\Gamma_C^a$  and  $\Gamma_C^b$  respectively the two boundaries which are opposite and represent the potential contact between the two electrodes. We denote by  $\underline{n}^\ell$  the outward normal vector and by  $\underline{t}^\ell$  the tangential vector such that  $(\underline{t}^\ell, \underline{n}^\ell)$  is a positive oriented basis of  $\Omega^\ell$ ,  $\ell = 1, 2$ .

Since the contact boundaries are not fixed, we shall introduce a common parametrization of the contact interface. To this end, we begin to consider the initial situation where two bodies are not submitted to any constraint such that the potential contact area  $\Gamma_C^a$  is in front of the potential contact area  $\Gamma_C^b$  but no contact holds. To characterize  $\Gamma_C^a$  and  $\Gamma_C^b$

we introduce a local parametrization of the two boundaries  $\underline{\chi}^a$  and  $\underline{\chi}^b$  defined on interval  $I = [0, 1]$  by

$$\begin{aligned} \underline{\chi}^a : I &\rightarrow \Gamma_C^a; & \underline{\chi}^b : I &\rightarrow \Gamma_C^b; \\ \xi &\mapsto \underline{\chi}^a(\xi) & \xi &\mapsto \underline{\chi}^b(\xi). \end{aligned} \quad (1)$$

For instance, we denote by  $\underline{n}^a = \underline{n}(\underline{\chi}^a(\xi))$  and  $\underline{n}^b = \underline{n}(\underline{\chi}^b(\xi))$  the respective parametrization of the outward normal vectors of  $\Gamma_C^a$  and  $\Gamma_C^b$ . Since the electrode have a small curvature with respect to the dimension of the electrode, we assume that they are collinear to the  $Ox_2$  with  $\underline{n}^a + \underline{n}^b = 0$ .

In the other hand, the interface displacements are perpendicularly and any contact point  $Y = (y_1, y_2)$ , in the new configuration when one applies forces, corresponds to a point  $X^a = (x_1^a, x_2^a) \in \Gamma_C^a$  and a point  $X^b = (x_1^b, x_2^b) \in \Gamma_C^b$  such that  $x_1^a = x_1^b = y_1$ , in the initial configuration. At last, we denote by  $g$  the initial gap between the two electrodes defined on  $I$  given by

$$g(\xi) = (\underline{\chi}^a(\xi) - \underline{\chi}^b(\xi)) \cdot \underline{n}^b(\xi). \quad (2)$$

## 2.1 MECHANICAL PROBLEM

We assume that the two bodies are elastic and we denote by  $\underline{\underline{\varepsilon}}(\underline{u})$  the strain tensor for any displacement  $\underline{u}(x)$  with respect to  $x$  in the initial configuration. The conservation of the impulsion reads

$$-\operatorname{div} \underline{\underline{\sigma}}(\underline{u}) = \underline{f} \text{ in } \Omega$$

where  $\underline{f}$  represents the body force. In our case,  $\underline{f}$  will be constituted by the gravity and the Laplace forces. Using the classical elasticity framework for isotropic linear material with the Hooke's law, the stress tensor writes

$$\underline{\underline{\sigma}} = \underline{\underline{\sigma}}(\underline{u}) = (\lambda \operatorname{tr}(\underline{\underline{\varepsilon}}(\underline{u})) \mathbb{I} + 2\mu \underline{\underline{\varepsilon}}(\underline{u})), \quad (3)$$

where  $\mathbb{I}$  denotes the 2-identity matrix, and the Lamé positive constants  $\lambda$  and  $\mu$  are given by (cf [4])

$$\mu = \frac{E}{2(1+\nu)} \text{ and } \lambda = \frac{E\nu}{(1+\nu)(1-2\nu)},$$

with the Young's modulus  $E > 0$  and the Poisson ratio  $\nu \in ]0, 1/2[$ . At the lateral sides

$\Gamma^a$  and  $\Gamma^b$ , no force and displacement are prescribed so we state  $\underline{\underline{\sigma}} \cdot \underline{n}^\ell = \underline{0}$  on  $\Gamma_L^a \cup \Gamma_L^b$ . The bottom part of the electrode is fixed so we required that no displacement occur and we state  $\underline{u} = \underline{0}$  on  $\Gamma_B$ . The upper part is controlled by the spring and the normal force is governed by

$$\underline{n}^{aT} \underline{\underline{\sigma}} \cdot \underline{n}^a = -\kappa(\underline{u} \cdot \underline{n}^a + \alpha)$$

where  $-\kappa\alpha$  is the initial force applied to the electrode while  $-\kappa(\underline{u} \cdot \underline{n}^a)$  represents the force due to the displacement. Moreover we require that no lateral movement takes place, so we state  $\underline{u} \cdot \underline{t} = 0$  on  $\Gamma_U$  to prevent the horizontal movement.

Now we deal with the contact interface condition. For a given configuration (spring and body force ) the interfaces  $\Gamma_C^a$  and  $\Gamma_C^b$  move and we obtain two new interfaces  $\hat{\Gamma}_C^a$  and  $\hat{\Gamma}_C^b$  which are partially in contact and the new configuration presents a commune interface

$$\mathcal{A} = \hat{\Gamma}_C^a \cap \hat{\Gamma}_C^b.$$

The active set is characterized by the interval  $J$ , such that for any  $\xi \in J$ :

$$(\underline{u}^a \cdot \underline{n}^a) \circ \underline{\chi}^a(\xi) + (\underline{u}^b \cdot \underline{n}^b) \circ \underline{\chi}^a(\xi) = g(\xi), \quad (4)$$

and

$$(\underline{t}^{aT} \underline{\sigma}(\underline{u}^a) \underline{n}^a) \circ \underline{\chi}^a(\xi) = (\underline{t}^{bT} \underline{\sigma}(\underline{u}^b) \underline{n}^b) \circ \underline{\chi}^b(\xi) = 0, \quad (5)$$

$$(\underline{n}^{aT} \underline{\sigma}(\underline{u}^a) \underline{n}^a) \circ \underline{\chi}^a(\xi) = (\underline{n}^{bT} \underline{\sigma}(\underline{u}^b) \underline{n}^b) \circ \underline{\chi}^b(\xi) < 0. \quad (6)$$

On the free part of the interface, characterized by  $\xi \in I \setminus J$ , (no contact) we have:

$$\begin{aligned} (\underline{u}^a \cdot \underline{n}^a) \circ \underline{\chi}^a(\xi) + (\underline{u}^b \cdot \underline{n}^b) \circ \underline{\chi}^b(\xi) &< g(\xi) \\ (\underline{n}^{aT} \underline{\sigma}(\underline{u}^a) \underline{n}^a) \circ \underline{\chi}^a(\xi) &= (\underline{n}^{bT} \underline{\sigma}(\underline{u}^b) \underline{n}^b) \circ \underline{\chi}^b(\xi) = 0 \\ (\underline{t}^{aT} \underline{\sigma}(\underline{u}^a) \underline{n}^a) \circ \underline{\chi}^a(\xi) &= (\underline{t}^{bT} \underline{\sigma}(\underline{u}^b) \underline{n}^b) \circ \underline{\chi}^b(\xi) = 0 \end{aligned}$$

Note that the contact boundary is unknown and  $J$  has to be also determined.

## 2.2 ELECTRICAL PROBLEM

We model the current density  $\underline{J}^\ell$ , the electrical field  $\underline{E}^\ell$  and the scalar electrical potential  $V_e^\ell$  in each electrodes,  $\ell \in \{a, b\}$  by

$$\underline{E}^\ell = -\underline{\text{grad}} V_e^\ell, \quad \underline{J}^\ell = \sigma \underline{E}^\ell,$$

to obtain the classical potential formulation

$$-\nabla \cdot (\sigma \nabla V_e^\ell) = 0, \quad (7)$$

with  $\sigma$  represents the electrical conductivity. We prescribe the current of intensity  $I_0$  on boundary  $\Gamma_U$  and assume a uniform repartition of the density current such that we have  $\underline{J}^a \cdot \underline{n}^a = \frac{I_0}{|\Gamma_U|}$  on  $\Gamma_U$  where  $|\Gamma_U|$  represent the length of the interface.

We also prescribe the null potential on the bottom interface setting  $V_e^b = 0$  on  $\Gamma_B$ . At last, since no current crosses the lateral interfaces, we set  $\frac{\partial V_e^\ell}{\partial \underline{n}} = 0$  on  $\Gamma_L^\ell$ .

Since we solve the scalar potential in each sub-domain, we have to prescribe the electrical condition on the active subset and the free subset for the contact interface. As for the lateral side, we prescribe  $\frac{\partial V_e^\ell}{\partial \underline{n}} = 0$  on  $\Gamma_C^\ell \setminus \mathcal{A}$  while we enforce the continuity of the electrical potential and the current on the active set

$$V_e^b - V_e^a = 0 \quad \text{on } \mathcal{A} \quad (8)$$

$$\underline{J}^b \cdot \underline{n}^b + \underline{J}^a \cdot \underline{n}^a = 0 \quad \text{on } \mathcal{A}. \quad (9)$$

### 2.3 MAGNETIC PROBLEM

The calculation of the magnetic field  $\underline{B}$  of current system is carried out with the BiotSavart formula for two-dimensional geometries  $\Omega \in \mathbb{R}^2$  as [6]. The magnetic field at a point  $\underline{x}$  is given by

$$\underline{B}(\underline{x}) = -\frac{1}{2\pi} \int_{\Omega} \underline{j}(\underline{y}) \wedge \nabla \ln(|\underline{y} - \underline{x}|) d\underline{y}, \quad (10)$$

for a current  $\underline{j}$  flowing in the direction of  $\vec{e}_1$  and  $\vec{e}_2$ . Equation (10) writes

$$\underline{B}(\underline{x}) = \frac{\vec{e}_3}{2\pi} \int_{\Omega} \frac{\det[\underline{j}(\underline{y}), (\underline{x} - \underline{y})]}{|\underline{x} - \underline{y}|^2} d\underline{y}. \quad (11)$$

### 3 DISCRETISATION AND NUMERICAL METHODS

Let us denote by  $\mathcal{T}_h^\ell$  the triangulation in cell  $C$  of the domain  $\Omega^\ell$  with  $\ell = a, b$  and  $\mathcal{T}_h = \mathcal{T}_h^a \cup \mathcal{T}_h^b$ . In this study, we assume that the two domains are symmetric such that the nodes on the on each contact zone  $\Gamma_C^a$  and  $\Gamma_C^b$  correspond and we introduce the interval  $I$  to provide a common parametrization of the two contacts interfaces.  $\mathcal{M}_h$  denote the mesh of interval  $I$  such that the nodes of  $I$ ,  $\Gamma_C^a$  and  $\Gamma_C^b$  corresponds. In future works, we intend to remove this constraint employing the Mortar technique [1, 2] or the three-field domain decomposition method [3].

#### 3.1 MECHANICAL PROBLEM

At rest, the two contact interfaces are given by the  $\underline{\chi}^\ell(\xi)$  functions from which we deduce the gap function (2). The configuration at rest correspond to the reference configuration. After applying the spring pressure, the gravity and the Lorentz-Laplace forces, we obtain a new configuration characterized (in the reference configuration) by an active zone  $\mathcal{A}^\ell \subset \Gamma_C^\ell$ . One has to provide the active zone such that relations (4) and (5) have to be both satisfied with the constraint condition (6).

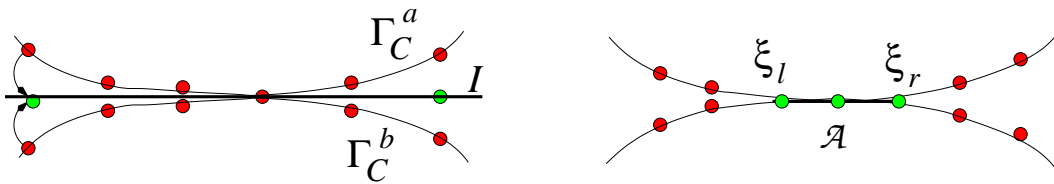


Figure 3: The contact zone: before applying forces (left), after applying forces (right)

To solve the mechanical problem, we use a domains decomposition technique [5]. To this end, we denote by  $\mathcal{A}_k^\ell \subset \Gamma_C^\ell$  a candidate for the active zone characterized by  $J^k = [\xi_l^k, \xi_r^k]$  where  $\underline{\chi}^\ell(\xi_l^k)$  correspond to two opposite nodes of  $\Gamma_C^\ell$  on the left of the contact zone and  $\underline{\chi}^\ell(\xi_r^k)$  correspond to two opposite nodes on the right.

### 3.1.1 The Lagrange Multiplier problems

For the meshes  $\mathcal{T}_h^a$ ,  $\mathcal{T}_h^b$  and  $\mathcal{M}_h$  we consider the associated discrete spaces

$$\begin{aligned}\mathbb{V}_h^a &= \{\underline{\varphi} = (\varphi_1, \varphi_2) \text{ continuous linear piecewise on } \Omega_a \text{ such that } (\varphi_1)|_{\Gamma_U} = 0\}, \\ \mathbb{V}_h^b &= \{\underline{\varphi} = (\varphi_1, \varphi_2) \text{ continuous linear piecewise on } \Omega_b \text{ such that } (\underline{\varphi})|_{\Gamma_B} = (0, 0)^T\}, \\ \mathbb{W}_h(J^k) &= \{\psi \text{ continuous linear piecewise on } J^k\}.\end{aligned}$$

Moreover, for any  $\psi \in \mathbb{W}_h(J^k)$ ,  $\Pi_\ell^k(\psi)$  denotes the projection of  $\psi$  on the contact boundaries  $\mathcal{A}_k^\ell$  such that  $\Pi_\ell^k(\psi)(P) = 0$  for all the nodes in  $\Gamma_C^\ell \setminus \mathcal{A}_k^\ell$ . We propose the iterative procedure to determine the configuration when enforcing relations (4) and (5). To this end, we denote by  $U_n \in \mathbb{W}_h(J^k)$  a given normal displacement on  $J^k$ , we consider the Lagrangian augmented problem, for  $\underline{\varphi} \in \mathbb{V}_h^a$

$$\int_{\Omega_a} \underline{\underline{\sigma}}(\underline{u}_h) : \underline{\underline{\varepsilon}}(\underline{\varphi}) \, d\underline{x} + \kappa \int_{\Gamma_U} (\underline{u}_h^a \cdot \underline{n}^a)(\underline{\varphi} \cdot \underline{n}^a) \, ds = \int_{\Omega_a} \underline{f} \cdot \underline{\varphi} \, d\underline{x} + \kappa \alpha \int_{\Gamma_U} (\underline{\varphi} \cdot \underline{n}^a) \, ds + \int_{\mathcal{A}_k^a} \Pi_a^k(\lambda_h^a) \varphi_2 \, ds$$

where  $\lambda_h^a$  is Lagrange multiplier associated to the normal displacement constraint, for all  $\psi \in \mathbb{W}_h$

$$\int_{\mathcal{A}_k^a} (\underline{u}_h^a \cdot \underline{n}^a) \Pi_a^k(\psi) \, ds = \int_{J^k} U_n \psi \, d\xi.$$

The second Lagrangian augmented problem writes for all  $\underline{\varphi} \in \mathbb{V}_h^b$

$$\int_{\Omega_b} \underline{\underline{\sigma}}(\underline{u}_h) : \underline{\underline{\varepsilon}}(\underline{\varphi}) \, d\underline{x} = \int_{\Omega_b} \underline{f} \cdot \underline{\varphi} \, d\underline{x} + \int_{\mathcal{A}_k^b} \Pi_b^k(\lambda_h^b) \varphi_2 \, ds$$

where  $\lambda_h^b$  is Lagrange multiplier associated to the normal displacement constraint, for all  $\psi \in \mathbb{W}_h$

$$\int_{\mathcal{A}_k^b} (\underline{u}_h^b \cdot \underline{n}^b) \Pi_b^k(\psi) \, ds = \int_{J^k} (g - U_n) \psi \, d\xi$$

to satisfy condition (4). The contact problem is solved if one can determine the normal displacement  $U_n$  such that  $\lambda_h^a = \lambda_h^b$  on  $J^k$ .

### 3.1.2 Resolution of the contact problem for $J^k$ given

We proceed with the description of the iterative procedure to solve the contact problem. Let  $U_n^{(m)}$  be a predicted displacement, we compute the associated Lagrange multipliers  $\lambda_h^a$  and  $\lambda_h^b$  given by section 3.1.1. Then we consider the two problems

$$\int_{\Omega_a} \underline{\underline{\sigma}}(\underline{w}_h^a) : \underline{\underline{\varepsilon}}(\underline{\varphi}) \, d\underline{x} + \kappa \int_{\Gamma_U} (\underline{w}_h^a \cdot \underline{n}^a)(\underline{\varphi} \cdot \underline{n}^a) \, ds = \int_{\mathcal{A}_k^a} \Pi_a^k(\lambda_h^a - \lambda_h^b) \varphi_2 \, ds$$

and

$$\int_{\Omega_b} \underline{\underline{\sigma}}(\underline{w}_h^b) : \underline{\underline{\varepsilon}}(\underline{\varphi}) \, d\underline{x} = \int_{\mathcal{A}_k^b} \Pi_b^k(\lambda_h^a - \lambda_h^b) \varphi_2 \, ds.$$

We then set for each node  $\xi_j$  of  $\mathcal{M}_h$

$$U_n^{(m+1)}(\xi_j) = U_n^{(m)}(\xi_j) - \frac{\theta}{2} \left[ (\underline{w}_h^a \cdot \underline{n}^a) \circ \chi^a(\xi_j) + (\underline{w}_h^b \cdot \underline{n}^b) \circ \chi^b(\xi_j) \right].$$

For  $\theta > 0$  small enough, the procedure converges to the solution (see [5]).

### 3.1.3 Determination of $J$

For a given  $J^k$  we solve the contact problem but the constraint (6) which predict a negative normal stress on the contact is not necessary achieved. The strategy consists in taking  $J^0 = I$  as the initial guess and if (6) is not satisfied with  $J^k$ , we reduce the domain removing the first and the last node of  $J^k$  to construct  $J^{k+1}$ .

## 3.2 ELECTRICAL PROBLEM

We now assume that the active zone  $\mathcal{A}$  is given and we consider two sub-problems and we denote by  $V_h$  the interface potential at the contact zone define on  $\mathcal{A}$  as a continuous linear piecewise function. We formulate the discrete problem in the following way.

Find  $V_h^a$  continuous, linear piecewise on  $\Omega^a$  such that

$$\int_{\Omega^a} \nabla V_h^a \cdot \nabla \phi \, d\underline{x} = \int_{\Gamma_U} \underline{J}^a(s) \phi(s) \, ds \quad (12)$$

with  $V_h^a = V$  on  $\mathcal{A}$ . To satisfy to current density continuity, we consider the second problem find  $V_h^b$  continuous, linear piecewise on  $\Omega^b$  such that

$$\int_{\Omega^b} \nabla V_h^b \cdot \nabla \phi \, d\underline{x} = - \int_{\mathcal{A}} \sigma \nabla V_h^a \cdot \underline{n}^b \quad (13)$$

with  $V_h^b = 0$  on  $\Gamma_B$ .

We then deduce the voltage  $V_h \rightarrow G(V_h) = V_h^b$  on  $\mathcal{A}$  which provide a one-to-one map on the nodes of  $\mathcal{A}$ .

The solution of the electrical problem is reached when  $G(V_h) = V_h$  and we solve the fix point problem using the iterative procedure

$$V_h^{k+1} = \frac{V_h^k + G(V_h^k)}{2} \quad (14)$$

setting  $V_h^0 = 0$ .



### 3.3 MAGNETIC PROBLEM

Let  $\underline{j}^\ell = \sigma \nabla V_h^\ell$  the constant piecewise approximation of the density current on each cell and  $P_i$  a node of the mesh. We compute the magnetic field at the node with

$$\underline{B}_i = \underline{B}(P_i) = \frac{\vec{e}_3}{2\pi} \sum_{C_k \in \mathcal{T}_h} |C_k| \frac{\det[\underline{j}(M_k), M_k P_i]}{|M_k P_i|^2}$$

where  $M_k$  is the centroid of cell  $C_k$ ,  $|C_k|$  the cell area and  $\underline{j}(M_k)$  the constant vector in  $C_k$ . From the magnetic field, we deduce an approximation of the Lorentz-Laplace force

$$\underline{f}(P_i) = \sigma \underline{E}(P_i) \wedge \underline{B}_i$$

where  $\underline{E}(P_i)$  is an interpolation at node  $P_i$  with the piecewise constant vectors  $\underline{E}_k = \nabla V_h|_{C_k}$  on the neighbour cells.

## 4 NUMERICAL RESULTS

We present some numerical results obtained with the schemes presented in the previous section. We consider a problem where the gravity and the Lorentz-Laplace forces can be neglected with respect to the spring pressure characterized by  $\kappa = 10^8$  and  $\alpha = -0.05$ . We first solve the contact problem to determine the active zone  $\mathcal{A}$ . Figure 4 shows the displacement vectors for the two elastic bodies (left) and we present on the right a zoom in the contact zone. From the contact interface previously computed by the mechanical

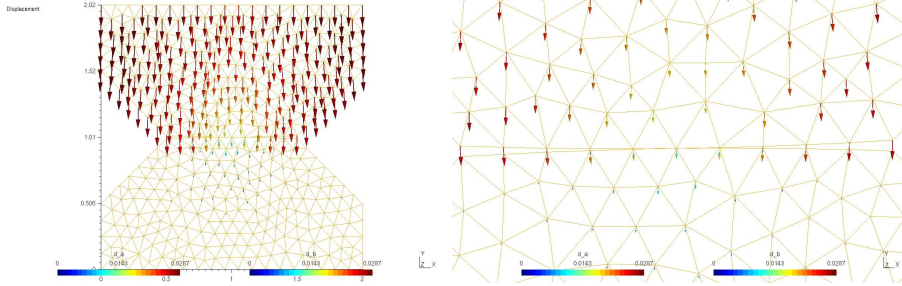


Figure 4: Displacement : global view (left), zoom at the contact interface (right)

problem, we solve the density current problem where we prescribe  $I_0 = 20 \text{ kA}$ . Figure 5 gives the density current distribution in the two domains and the zoom view clearly shows the half loop of the electric current in the vicinity of the contact zone which is responsible for the repulsion forces.

In figure 6, we plot the  $e_3$  component of the magnetic field. Since the current flows to the bottom, we check that the magnetic field is positive on the left side (red area) and negative on the right side (blue area).

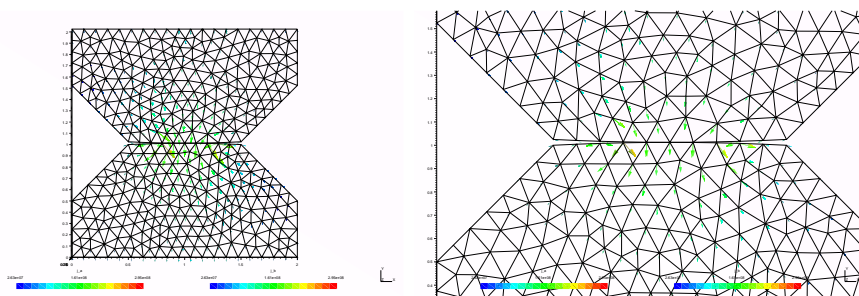


Figure 5: Current density distribution : global view (left), zoom at the contact interface (right)

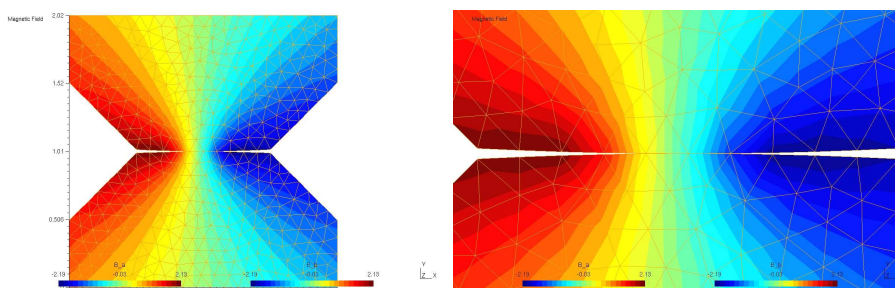


Figure 6: Magnetic field distribution (componant following  $e_3$ ):global view (left), zoom at the contact interface (right)

## 5 CONCLUSIONS

We have presented a two-dimensional model of the vacuum disjuncteur where we have taken into account the mechanical, the electrical and the electromagnetic problems. Numerical schemes have been designed to compute an approximation for each sub-problem. The next step consists in linking the three sub-problems via the Laplace-Lorentz force to provide the equilibrium solution for a high current intensity where the repulsive force are predominant to determine the contact area.

## REFERENCES

- [1] F. Ben Belgacem, *The mortar finite element method with Lagrange multipliers*, Numerische Mathematik 84 (1999), n. 2, pp 173-197.
- [2] C. Bernardi, Y. Maday, and A. Patera. A new non conforming approach to domain decomposition: The mortar element method. In H. Brezzi et al., editor, *Nonlinear partial differential equations and their applications*, pages 13-51. Paris, 1994.
- [3] F. Brezzi and L. D. Marini, *Macro hybrid elements and domain decomposition methods*, Optimization et Côtrole (J. A. Désideri, L. Fezoui, B. Larrouturou, and B.

- Rousselet, eds.), 1993, pp. 89-96.
- [4] G. Duvaut and J. L. Lions, *Les inéquations en mécanique et en physique* Dunod, Paris, 1972
- [5] J. Haslinger, R. Kučera, T. Sassi, *A domain decomposition algorithm for contact problems: analysis and implementation*, Math. Model. Nat. Phenom. Vol 4, No 1 (2009) 123–146.
- [6] J.-C. Suh, *The evaluation of the Biot-Savart integral*, Journal of Engineering Mathematics Vol 37 (2000) 375–395.